1521-0103/382/2/66–78$35.00
THE JOURNAL OF PHARMACOLOGY AND EXPERIMENTAL THERAPEUTICS

dx.doi.org/10.1124/jpet.121.001033
J Pharmacol Exp Ther 382:66–78, August 2022

The Nonpeptide Agonist MK-5046 Functions As an Allosteric Agonist for the Bombesin Receptor Subtype-3

Irene Ramos-Alvarez, Tatiana Iordanskaia, Samuel A. Mantey, and Robert T. Jensen

Digestive Diseases Branch, National Institute of Diabetes and Digestive and Kidney Diseases, National Institutes of Health, Bethesda, Maryland

Received November 22, 2021; accepted May 5, 2022

ABSTRACT

Allosteric ligands of various G-protein–coupled receptors are being increasingly described and are providing important advances in the development of ligands with novel selectivity and efficacy. These unusual properties allow expanded opportunities for pharmacologic studies and treatment. Unfortunately, no allosteric ligands are yet described for the bombesin receptor family (BnRs), which are proposed to be involved in numerous physiologic/pathophysiological processes in both the central nervous system and peripheral tissues. In this study, we investigate the possibility that the bombesin receptor subtype-3 (BRS-3) specific nonpeptide receptor agonist MK-5046 [(2S)-1,1,1-trifluoro-2-[4-(1H-pyrazol-1-yl)phenyl]-3-(4-[[1-(trifluoromethyl) cyclopropyl]methyl]-1H-imidazol-2-yl)propan-2-ol] functions as a BRS-3 allosteric receptor ligand. We find that in BRS-3 cells, MK-5046 only partially inhibits iodine-125 radionuclide (^{125}I)-Bantag-1 [Boc-Phe-His-4-amino-5-cyclohexyl-2,4,5-trideoxypentonyl-Leu-(3-dimethylamino) benzylamide N-methylammonium trifluoroacetate] binding and that both peptide-1 (a universal BnR-agonist) and MK-5046 activate phospholipase C; however, the specific BRS-3 peptide antagonist Bantag-1 inhibits the action of peptide-1 competitively, whereas for MK-5046 the inhibition is noncompetitive and yields a curvilinear Schild plot. Furthermore, MK-5046 shows other allosteric behaviors, including slowing dissociation of the BRS-3 receptor ligand ^{125}I-Bantag-1, dose-inhibition curves being markedly affected by increasing ligand concentration, and MK-5046 leftward shifting the peptide-1 agonist dose-response curve. Lastly, receptor chimeric studies and site-directed mutagenesis provide evidence that MK-5046 and Bantag-1 have different binding sites determining their receptor high affinity/selectivity. These results provide evidence that MK-5046 is functioning as an allosteric agonist at the BRS-3 receptor, which is the first allosteric ligand described for this family of receptors.

SIGNIFICANCE STATEMENT

G-protein–coupled receptor allosteric ligands providing higher selectivity, selective efficacy, and safety that cannot be obtained using usual orthosteric receptor-based strategies are being increasingly described, resulting in enhanced usefulness in exploring receptor function and in treatment. No allosteric ligands exist for any of the mammalian bombesin receptor (BnR) family. Here we provide evidence for the first such example of a BnR allosteric ligand by showing that MK-5046, a nonpeptide agonist for bombesin receptor subtype-3, is functioning as an allosteric agonist.

Introduction

The human bombesin receptor (BnR) family consists of three closely related receptors: the gastrin-releasing peptide receptor (GRPR), the neuromedin B receptor (NMBR), and the orphan receptor bombesin receptor subtype-3 (BRS-3) (Jensen et al., 2008). Numerous studies provide evidence that GRPR/NMBR are involved in a wide range of physiologic and pathophysiological processes, with gastrin-releasing peptide/neuromedin B (GRP/NMB) frequently functioning as neurotransmitters, as well as in an autocrine, paracrine, and neurocrine manner (Jensen et al., 2008, 2017). These include such diverse physiologic processes as being potent stimulants of growth/differentiation of various normal tissues; stimulating exocrine secretion as well as the release of numerous hormones; stimulating smooth muscle contraction/motility, particularly in the gastrointestinal (GI)/urogenital system; having potent effects in the immune and reproductive systems and in metabolic regulation; and having a wide range of peripheral/central nervous system (CNS) effects, including thermoregulation, behavioral, regulating circadian rhythm, sighing, and satiety (Jensen et al., 2008, 2017; Qu et al., 2018; Battey et al., 2021; Moody et al., 2021). Possible

This work was partially supported by intramural funds from National Institutes of Health National Institute of Diabetes and Digestive and Kidney Diseases [Grant DK053200-29] (to R.T.J.).
The authors declare that there are no conflicts of interest with the contents of this article.
dx.doi.org/10.1124/jpet.121.001033.

ABBREVIATIONS: Balb 3T3, Balb 3T3 mouse fibroblast; Bantag-1, Boc-Phe-His-4-amino-5-cyclohexyl-2,4,5-trideoxypentonyl-Leu-(3-dimethylamino) benzylamide N-methylammonium trifluoroacetate; Bn, bombesin; BnR, bombesin receptor; BRS-3, bombesin receptor subtype-3; CNS, central nervous system; D-PT-SP, (D-Pro^4, D-Trp^{7,9,10})-Substance P-(4–11); EC, extracellular domain of receptor; GI, gastrointestinal; GPCR, G-protein–coupled receptor; GRP, gastrin-releasing peptide; GRPR, gastrin-releasing peptide receptor; hBRS-3, human BRS-3; ^{125}I, iodine-125 radionuclide; IP, inositol phosphate; MK-5046, [(2S)-1,1,1-trifluoro-2-[4-(1H-pyrazol-1-yl)phenyl]-3-(4-[[1-(trifluoromethyl)cyclopropyl]methyl]-1H-imidazol-2-yl)propan-2-ol]; NMB, neuromedin B; NMBR, neuromedin B receptor; peptide-1, [D-Tyr^6, β-Ala^{11}, Phe^{13}, Nle^{14}]Bn-(6–14); PLC, phospholipase C.

pathophysiological roles of GRPR/NMBR receiving particular attention include being one of the G-protein–coupled receptors (GPCRs) most frequently overexpressed by many common tumors (breast, prostate, colon, pancreas, lung, CNS); having potent tumor growth effects, frequently in an autocrine manner; being the principal neurotransmitters mediating pruritis; and having possible roles in a number of other CNS disorders (Alzheimer's, memory dysfunction, schizophrenia) (Gonzalez et al., 2008b; Jensen et al., 2008; Sancho et al., 2011; Roesler and Schwartsmann, 2012; Ramos-Álvarez et al., 2015; Weber, 2015; Moreno et al., 2016; Moody et al., 2018, 2021; Battey et al., 2021). In contrast to GRPR/NMBR, only limited insights into possible roles of BRS-3 in physiologic/pathologic processes are available and are almost entirely from BRS-3 receptor knockout studies (Ohki-Hamazaki et al., 1997; Jensen et al., 2008; Feng et al., 2011; González et al., 2015; Xiao and Reitman, 2016; Li et al., 2019). These studies show that BRS-3 is particularly important in control of various behaviors, energy homeostasis, insulin/glucose regulation, feeding behavior, and body temperature control because these animals develop hypertension, obesity, diabetes, altered behavior, reduced metabolic rates, and altered satiety (Ohki-Hamazaki et al., 1997; Feng et al., 2011; Majumdar and Weber, 2012a,b; González et al., 2015; Ramos-Álvarez et al., 2015).

Recent studies have described, for a number of different receptor subtypes, the value of identifying allosteric ligands, which have several advantages over the native orthosteric receptor ligands, for studying the pharmacology of these receptors as well as studying their roles in various physiologic/pathophysiological processes (Cawston et al., 2012; Christopoulos, 2014; Nickols and Conn, 2014; van Westen et al., 2014). These advantages include greater receptor specificity for closely related receptor subtypes, greater safety because of ceiling effects to their responses, and potential for biased signaling (Cawston et al., 2012; Christopoulos, 2014; van Westen et al., 2014; Wold and Zhou, 2018). Even though allosteric modulators have been recognized for a number of G-protein–coupled receptors (GPCRs) (Christopoulos and Kenakin, 2002; May et al., 2004, 2007; Christopoulos, 2014; Khoury et al., 2014; Wootten et al., 2017; Wootten and Miller, 2020), including for a few gastrointestinal hormone/neurotransmitter receptors (Gao et al., 2008; Khoury et al., 2014; Dong et al., 2015; Wootten and Miller, 2020), and even though numerous different chemical classes of receptor agonists/antagonists (i.e., peptides, peptoids, nonpeptides) have been described for BnRs (Heinz-Erian et al., 1987; Coy et al., 1989; von Schrenck et al., 1990; Wang et al., 1990a,b; Jensen et al., 2008; Ramos-Álvarez et al., 2015; Moreno et al., 2016; Battey et al., 2021), none have been reported to function as an allosteric ligand for BRS-3 or the other BnR receptors (i.e., GRPR/NMBR).

The lack of allosteric ligands, with their enhanced specificity and other properties, for BnRs is a potential important limitation because the roles of BnRs in the above physiologic/pathologic processes or in treatment approaches have not been well defined. This has occurred because of the lack of high-affinity, specific agonist/antagonists that distinguish each BnR subtype, especially ligands that are nonpeptides. In the case of BRS-3, except for its role in satiety, temperature control, and energy/glucose metabolism defined from BRS-3 knockout mice studies, its possible roles in other physiologic/pathophysiological processes are largely unknown (Ohki-Hamazaki et al., 1997; Jensen et al., 2008; Feng et al., 2011; Majumdar and Weber, 2012a,b; González et al., 2015; Ramos-Álvarez et al., 2015; Xiao and Reitman, 2016; Qin and Qu, 2021). With the lack of a physiologic ligand, the development of pharmacologic tools to study this receptor have been challenging. However, because of its potential importance in satiety/obesity/diabetes [all of which BRS-3 knockout animals develop (Ohki-Hamazaki et al., 1997; Feng et al., 2011)], there has been considerable interest in developing pharmacologic tools for BRS-3. A potent panhuman BnR receptor peptide agonist [D-Tyr^{6}, β-Ala^{11},Phe^{13},Nle^{14}]Bn-(6-14) (peptide-1) has been described (Mantey et al., 1997; Pradhan et al., 1998; Uehara et al., 2011; Ramos-Alvarez et al., 2019), but it lacks specificity. Furthermore, both the peptide antagonist Bantag-1 [Boc-Phe-His-4-amino-5-cyclohexyl-2,4,5-trideoxypentonyl-Leu-(3-dimethylamino) benzylamide N-methylammonium trifluoroacetate] as well as two classes of potent nonpeptide agonists [i.e., MK-5046 (Sebhat et al., 2010; Guan et al., 2011; Reitman et al., 2012; Moreno et al., 2013) and various chiral diazepine analogs (Matsufuji et al., 2014; 2015; Ramos-Álvarez et al., 2016)] have recently been described. The latter group are the first potent nonpeptide agonists described for the BnRs. In a recent study (Ramos-Alvarez et al., 2019), the first specific BRS-3 radiolabeled antagonist-ligand, iodine-125 radionuclide (^{125}I)-Bantag-1, was described. In that study (Ramos-Alvarez et al., 2019), it was reported that saturable ligand binding was inhibited by the peptide agonist peptide-1 as well as by the peptide antagonist Bantag-1. In contrast, even with high concentrations of the nonpeptide agonist MK-5046 [(2S)-1,1,1-trifluoro-2-[4-(1H-pyrazol-1-yl)phenyl]-3-(4-[[1-(trifluoromethyl)cyclopropyl]methyl]-1H-imidazol-2-yl)propan-2-ol], saturable ligand binding to the BRS-3 cells was only partially inhibited, raising the possibility that MK-5046 could be binding to a different site and hence functioning in an allosteric manner and could thus be the first allosteric ligand of BnR family of receptors identified. The present studies were designed to explore this possibility in detail.

Materials and Methods

Materials

Balb 3T3 (Balb 3T3 mouse fibroblast) cells and the human lung cancer cells (NCI-N417) were purchased from the American Type Culture Collection (Gaithersburg, MD). Dulbecco's minimum essential medium (DMEM), RPMI 1640, phosphate-buffered saline (PBS), fetal bovine serum (FBS), Dulbecco's phosphate buffer saline (DPBS), trypsin-EDTA 1X, penicillin streptomycin, and Geneticin selective antibiotic (G418 Sulfate) were from Invitrogen (Carlsbad, CA). (D-Pro^{4}, D-Trp^{7,9,10})-Substance P-(4–11) (D-PT-SP), gastrin-releasing peptide (GRP), and neuromedin B (NMB) were from Bachem (Torrance, CA). The bombesin (Bn) analogs and [D-Tyr^{6}, β-Ala^{11}, Phe^{13}, Nle^{14}]Bn-(6-14) (peptide-1) (Mantey et al., 1997; Pradhan et al., 1998; Moreno et al., 2013) were obtained from Dr. David H. Coy (Tulane University, New Orleans, LA). Bombesin receptor subtype-3 antagonist Bantag-1 [Boc-Phe-His-4-amino-5-cyclohexyl-2,4,5-trideoxypentonyl-Leu-(3-dimethylamino) benzylamide N-methylammonium trifluoroacetate] (Guan et al., 2010; Feng et al., 2011; Moreno et al., 2013) was from Sigma-Aldrich (Allentown, PA). The BRS-3 nonagonist MK-5046 [(2S)-1,1,1-trifluoro-2-[4-(1H-pyrazol-1-yl)phenyl]-3-(4-[[1-(trifluoromethyl)cyclopropyl]methyl]-1H-imidazol-2-yl)propan-

2-ol] (Sebhat et al., 2010; Reitman et al., 2012; Moreno et al., 2013) and iodine-125 radionuclide [^{125}I] (10 mCi) (378 MBq) were from PerkinElmer Life Science (Boston, MA). Polyethylenimine (PEI) was from Polysciences, Inc. (Warrington, PA).

Methods

Stable Transfection. hBRS-3 stably transfected into Balb 3T3 cells were made as described previously (Benya et al., 1992, 1993, 1994, 1995; Ryan et al., 1998a). Balb 3T3 cells were grown overnight at 37°C in 10-cm tissue culture plates at the density of 2×10^6 cells per plate.

Cell Culture. Balb 3T3 cells stably expressing human BRS-3 (hBRS-3) receptor were grown in DMEM supplemented with 10% FBS and 300 mg/l G418 sulfate. The human lung cancer cells (NCI-N417) were grown in RPMI-1640 supplemented with 10% FBS.

Preparation of ^{125}I-Labeled Peptides. ^{125}I-Bantag-1, with specific activity of 2200 Ci/mmol, was prepared using Iodo-gen by a modification of methods described (von Schrenck et al., 1990; Mantey et al., 1993, 1997; Ramos-Alvarez et al., 2019). The free iodine-125 was separated by applying the reaction mixture onto a Sep-Pak, and the radiolabeled peptide was eluted with 60% acetonitrile in 0.1% trifluoroacetic acid (10 × 200 μl sequential elutions). The radioligand was purified with reverse-phase high-performance liquid chromatography (HPLC) using a μBondapak column (0.46 × 25 cm) from Waters Corporation as described previously (Ramos-Alvarez, et al., 2019). ^{125}I-peptide-1 (^{125}I-[D -Tyr^6, β-Ala^{11}, Phe^{13}, Nle^{14}]Bn-(6-14)), with a specific activity of 2200 Ci/mmol, was prepared as described previously (Mantey et al., 1997; González et al., 2009; Moreno et al., 2013; Nakamura et al., 2016).

Binding Studies to Cells. hBRS-3/BALB cells (1×10^6 cells/ml), NCI-N417 lung cells (5×10^6 cells/ml), or transiently transfected CHOP cells ($0.2–4 \times 10^6$ cells/ml) were incubated for 40–60 min. at 22°C with 50 pM ^{125}I-labeled ligands alone or with 1-10 μM unlabeled Bantag-1 or peptide-1 in 300 μl of binding buffer as described previously (Ryan et al., 1998a,b; Moreno et al., 2013; Nakamura et al., 2016; Ramos-Alvarez et al., 2019). The standard binding buffer contained 24.5 mM HEPES (pH 7.4), 98 mM NaCl, 6 mM KCl, 2.5 mM KH_2PO_4, 5 mM sodium pyruvate, 5 mM sodium fumarate, 5 mM sodium glutamate, 2 mM glutamine, 11.5 mM glucose, 0.5 mM $CaCl_2$, 1.0 mM $MgCl_2$, 0.01% (w/v) soybean trypsin inhibitor, 0.2% (v/v) amino acid mixture, 1% (w/v) bovine serum albumin Fraction V (BSA), and 0.05% (w/v) bacitracin. After the incubation, 100 μl of each sample was removed and processed as described previously (Ryan et al., 1998a,b; Moreno et al., 2013; Nakamura et al., 2016; Ramos-Alvarez et al., 2019). The amount of radioactivity bound to the cells was measured in a Wizard 1470 Automatic Gamma counter (Packard Instruments, Meriden, CT). Total binding was expressed as the percentage of total radioactivity that was associated with the cell pellet. Nonsaturable binding was <15% of the total binding in all experiments. Each point was measured in duplicate, and each experiment was replicated at least four times. Calculation of ligand receptor affinities was performed by determining the IC_{50} using the curve-fitting program Prism GraphPad 4.0 (GraphPad Software, Inc., La Jolla, CA).

Preparation of Membranes from hBRS-3/BALB Cells. hBRS-3/BALB cell membranes were prepared as described previously (Mantey et al., 1993; Tsuda et al., 1997) using a homogenizing buffer containing 50 nM Tris (pH 7.4), 0.2 mg/ml soybean inhibitor, 0.1% bacitracin, and 0.2 mg/ml benzamidine. hBRS-3/BALB cells (1×10^7 cell/ml) were homogenized for 30 seconds with a polytron (Brinkmann Instruments Inc., Westbury, NY) at speed 6 and centrifuged at 1500 rpm for 10 minutes. The supernatant was removed and recentrifuged at 15,000 rpm to pellet the membranes. The membranes were suspended in binding buffer and stored at −70°C until used.

Binding of ^{125}I-Bantag-1 to hBRS-3/BALB Membranes. hBRS-3/BALB cell membranes (from 1×10^7 cells/ml) were incubated in standard membrane binding buffer containing 10 mM HEPES [pH 7.4, 118 mM NaCl, 4.7 mM KCl, 5mM $MgCl_2$, 1 mM EGTA, 0.2 mg/ml benzamidine, 0.2 mg/ml soybean trypsin inhibitor, 0.1% bacitracin, and 0.2% (w/v) BSA]. Binding was as stated above with cells.

Measurement of [^{3}H]Inositol Phosphates. [^{3}H]Inositol phosphates (IPs) were determined as described previously. The total [^{3}H]IP was isolated by anion-exchange chromatography as described previously (Rowley et al., 1990; Benya et al., 1993; Moreno et al., 2013).

Preparation of GRPR Gain-of-Affinity Chimeric Receptors (GRPR-BRS-3 Chimeric Receptors) and BRS-3 Loss-of-Affinity Receptor (R127Q BRS-3 Point Mutant Receptor). Gain-of-affinity GRPR chimeric receptors were prepared by replacing the extracellular domains (EC1, EC2, and EC3) of GRPR one at a time by the comparable extracellular domains of BRS-3 [(ec1-BRS-3) GRPR, (ec2-BRS-3) GRPR, and (ec3-BRS-3) GRPR] as described previously (Tokita et al., 2001; Gonzalez et al., 2008a; Uehara et al., 2012; Nakamura et al., 2016). The loss-of-affinity BRS-3 receptor [(R127Q) BRS-3 point mutant] (replacing arginine in position 127 of BRS-3 by glutamine from a similar position in GRPR) was constructed using the QuikChange Site-Directed Mutagenesis Kit (Agilent Technologies, Santa Clara, CA) following the manufacturer's instructions with minor modifications as described previously (Gonzalez et al., 2008a; Uehara et al., 2012; Nakamura et al., 2016). BRS-3 receptor affinity was determined after transient transfection using lipofectamine of the above BnR chimeric and mutant receptors in CHOP cells followed by binding studies as described previously (Uehara et al., 2012; Nakamura et al., 2016).

Statistical Analysis. IC_{50}s from the binding data were obtained by curve fitting using Prism GraphPad 7.0 (nonlinear curve fitting). An analysis of variance was used to determine the statistical significance of differences in affinity of each Bn agonist/antagonist with changes showing ≥2-fold difference from control. In all experiments, cell concentrations were set such that <15% of total radioactivity was bound, and the amount of saturable ligand bound was similar in the control and chimeric receptor construct studies; therefore, in the statistical analysis, only two variables (i.e., each Bn agonist/antagonist and its own control, binding similar amount of ligand) were analyzed.

Results

Ability of Various Bombesin Ligands To Inhibit Binding of ^{125}I-Bantag-1 to hBRS-3/BALB Cells

To explore the comparative abilities of the nonpeptide BRS-3 agonist MK5046 (Fig. 1) and various BRS-3/BnR receptor ligands to directly interact with the hBRS-3 receptor, full dose-inhibition curves were performed with the BRS-3 specific antagonist ligand ^{125}I-Bantag-1 (Ramos-Alvarez et al., 2019) using both N417 lung cancer cells, which natively express hBRS-3 at low concentrations (Ryan et al., 1998b; Sancho et al., 2010), and hBRS-3 BALB–transfected cells, which have been shown to have similar pharmacology and signaling to native hBRS-3 cells (Markussen et al., 1996; Mantey et al., 1997; Jensen et al., 2008) (Fig. 2). Previous studies (Ryan et al., 1998b; Sancho et al., 2010; Moreno et al., 2013) have reported that even though N417 lung cancer cells possess native BRS-3 receptors at low concentrations, binding studies are possible if large numbers of cells (>5–10 × 10^6 cells/ml) are used in the binding assays; sufficient binding could then be obtained to perform detailed dose-inhibition curves and calculation of affinity constants for the different BRS-3 ligands in these cells. Studies were performed with cells possessing both native BRS-3 receptors and those expressed in transfected cells because previous studies on other receptors show that they may give differing results on assessing a ligand's possible allosteric interaction (Langmead and Christopoulos, 2006).

MK-5046

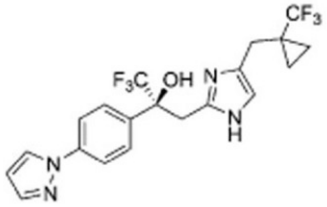

[(2S)-1,1,1-trifluoro-2-[4-(1H-pyrazol-1-yl)phenyl]-3-(4-{[1-(trifluoromethyl)cyclopropyl]methyl}-1H-imidazol-2-yl)propan-2-ol]

Bantag-1

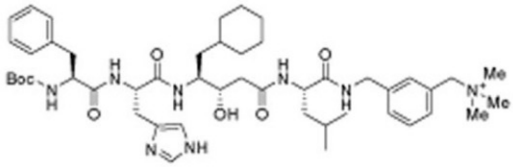

Boc-Phe-His-4-amino-5-cyclohexyl-2,4,5-trideoxypentonyl-Leu- (3-dimethylamino) benzylamide N-methylammonium trifluoroacetate

Peptide-1

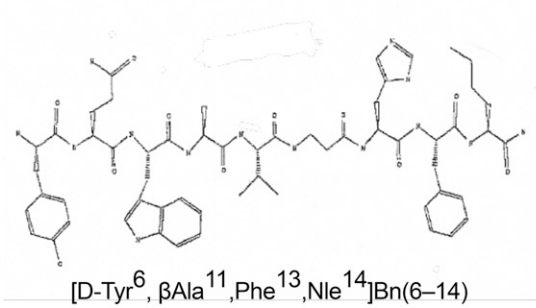

[D-Tyr^{6}, βAla^{11},Phe^{13},Nle^{14}]Bn(6–14)

[DTyr^{6}, Gln^{7}, Trp^{8}, Ala^{9}, Val^{10}, βAla^{11},His^{12}, Phe^{13},Nle^{14}]Bn(6–14)

Fig. 1. Structures of the BRS-3 selective nonpeptide agonist MK-5046, the BRS-3 selective antagonist Bantag-1, and the high-affinity BnR peptide agonist Peptide 1.

The two hBRS-3 antagonists (Bantag-1 and D-PT-SP) and the peptide agonist peptide-1 inhibited ^{125}I-Bantag-1 saturable binding by >90%–99% if sufficiently high concentrations could be used, whereas even at high concentrations (up to 10,000 nM) MK-5046 only partially inhibited binding by 40%–50% ± 2% (Fig. 2). Previous studies on both cells demonstrate that Bantag-1 can interact with both high- (20%) and low-affinity hBRS-3 binding sites (Moreno et al., 2013). These results suggest that the low-affinity antagonist D-PT-SP interacts with all ^{125}I-Bantag-1 sites and that the peptide agonist peptide-1, which induces the high-affinity state, interacts with >90%; however, the nonpeptide agonist MK5046 interacts with only 40% of the total sites that ^{125}I-Bantag-1 binds to. (Fig. 2; Table 1). These data demonstrate that Bantag-1 and MK-5046 are not largely sharing the same binding sites and raise the question of whether MK-5046 could be functioning as an allosteric agonist through binding to sites other than the orthosteric binding site. This could best be further directly investigated by using a radiolabeled MK-5046 analog to directly assess its interaction; unfortunately, no such radiolabeled ligand is currently available and

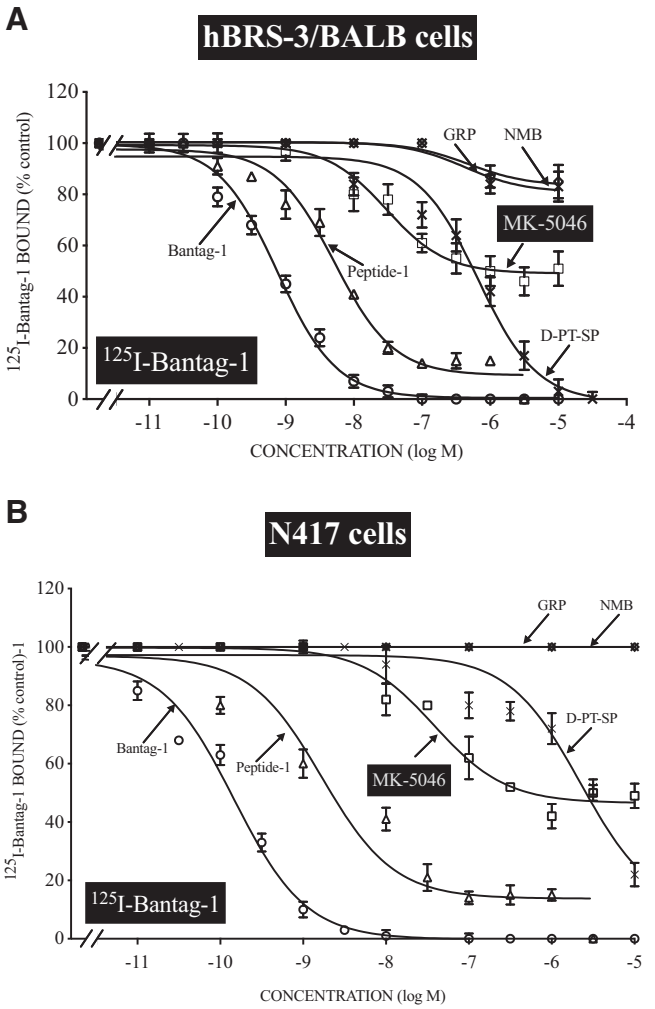

Fig. 2. Ability of various bombesin receptor ligands to inhibit binding of the radiolabeled antagonist ^{125}I-Bantag-1 to hBRS-3/BALB cells (1×10^6 cells/ml) (A) or to N417 lung cancer cells possessing native hBRS-3 (5×10^6 cells/ml) (B). hBRS-3/BALB or N417 cells were incubated with 50 pM ^{125}I-Bantag-1 with or without increasing concentrations of various unlabeled bombesin receptor ligands for 60 minutes at 22°C. Results are expressed as the percentage of saturable binding with no additions. The results are the mean and S.E.M. from at least three separate experiments, and in each experiment the data points were determined in duplicate.

fully characterized. Therefore, the purpose of the present study was to pharmacologically explore further the interaction of MK-5046 with hBRS-3 and assess whether it was interacting in an allosteric manner.

Ability of Increasing Concentrations of Bantag-1 To Affect the Dose-Response Curves for Activation of Phospholipase C and Generation of [^{3}H]IP by Either Peptide-1 or MK-5046

Previous studies (Ryan et al., 1998b; Jensen et al., 2008; Ramos-Álvarez et al., 2015; Alexander et al., 2019) demonstrate that stimulation of phospholipase C (PLC) is one of the principal intracellular signaling cascades with hBRS-3 activation, resulting in stimulation of phosphoinositide generation and elevation of cytosolic calcium levels. Both the BRS-3 peptide agonist peptide-1 and the nonpeptide agonist MK-5046 have been shown to activate both native and transfected BRS-3 in various cells, resulting in stimulation of phospholipase C (Mantey et al., 1997; Ryan et al., 1998a; Moreno et al., 2013, 2018). In BALB cells containing BRS-3 receptor, the peptide agonist peptide-1 as well as the nonpeptide agonist MK-5046 each activated PLC, stimulating generation of [^{3}H]IP, with peptide-1 being more potent (EC_{50}: 3.48 ± 0.02 nM) than MK-5046 (EC_{50}: 12.5 ± 1.1 nM) (Fig. 3).

TABLE 1

Comparison of affinities of various BnR agonists and antagonists for hBRS-3 containing cells determined from ^{125}I-Bantag-1 binding hBRS-3 stably transfected into BALB 3T3 cells (1×10^6 cells/ml) and NCI-N417 cells that contain native hBRS-3 (5×10^7 cells/ml) (Ryan et al., 1998b; Sancho et al., 2010) were incubated with 50 pM ^{125}I-Bantag-1 for 60 min at 22°C. In each experiment, each value was determined in duplicate and values given are mean and S.E.M. from at least three separate experiments. Data are calculated from dose-inhibition curves shown in Fig. 2 for each peptide using a nonlinear regression curve-fitting program (Prism). Each value is the mean ± S.E.M. from at least three experiments.

	K_i (nM) Cells	
	hBRS-3/BALB	NCI-N417
Peptide-1	0.68 ± 0.02	1.56 ± 0.88
Bantag-1	0.74 ± 0.01	0.16 ± 0.01
D-PT-SP	658 ± 0.6	2215 ± 0.13
MK-5046	30 ± 1.3	38 ± 1.3
NMB	>10,000	>10,000
GRP	>10,000	>10,000

K_i, inhibition constant.

Bantag-1 is reported to be a highly selective, potent peptide receptor antagonist of BRS-3 receptors in humans, rats, and mice (Guan et al., 2010; Feng et al., 2011; Moreno et al., 2013). To further assess the nature of the ability of the peptide antagonist Bantag-1 to alter cell activation stimulated by either the peptide agonist peptide-1 or the nonpeptide agonist MK-5046 by interacting with these agonists' binding sites (Ryan et al., 1998a; Jensen et al., 2008; Ramos-Álvarez et al., 2015), the effect of increasing concentrations of Bantag-1 on the dose-response curves for PLC activation and stimulation of the generation of inositol phosphates by these agonists was assessed (Fig. 3). Bantag-1 alone had no effect on [^{3}H]IP concentrations of up to 1 μM. Increasing concentrations of Bantag-1 caused a parallel rightward shift of the dose-response curve for the ability of peptide-1 to activate PLC and increase generation of phosphoinosites (EC_{50}s: 3.5, 6.5, 39, and 105 nM with 0, 1, 10, and 100 nM Bantag-1) without any change in the magnitude of maximal stimulation (Fig. 3A). With MK-5046, with increasing concentrations of Bantag-1, there was also a progressive rightward shift of the MK-5046 dose-response curve with 0 nM, 1 nM, 10 nM, and 100 nM Bantag-1 (EC_{50}s: 12, 19, 58, and 260 nM, respectively; Fig. 3B). However, in contrast to the lack of effect of increasing concentrations of Bantag-1 on maximal stimulation by peptide-1, its efficacy with MK-5046 was progressively reduced with 1 nM, 10 nM, and 100 nM Bantag-1, causing a respective 12%, 22%, and 42% reduction in maximal stimulation (Fig. 3B). These data demonstrate that Bantag-1 was functioning as a competitive antagonist at the peptide-1 binding sites, resulting in cell activation and PLC stimulation, but that at the MK-5046 binding sites responsible for cell activation, Bantag-1 was functioning in a noncompetitive manner. Schild plots of the inhibitory effect of Bantag-1 support this conclusion with a slope not significantly different from unity for peptide-1 (Fig. 3A, insert; slope: 0.97 ± 0.07); whereas with MK-5046 activation, the slope markedly differed from unity (Fig. 1B, insert; slope: 0.51 ± 0.18; $P < 0.05$) consistent with noncompetitive

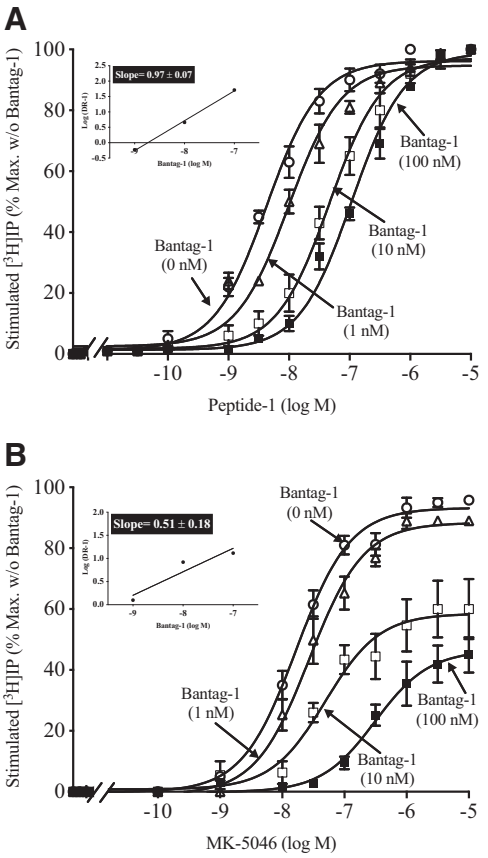

Fig. 3. Comparison of the ability of increasing concentrations of Bantag-1 (1–100 nM), a BRS-3 receptor antagonist, to alter the dose-response stimulation of [^{3}H]IP generation in hBRS-3/BALB by the BRS-3 peptide agonist peptide-1 (A) or the nonpeptide agonist MK-5046 (B). After loading the cells with 3 μCi/ml myo-[2-^{3} H]inositol by incubating overnight, cells were then washed and incubated with each agonist at the indicated concentration for 60 minutes at 37°C. The [^{3}H]IP measurement was determined as described in *Materials and Methods*. The results are the mean and S.E.M. from at least four separate experiments, and in each experiment the data points were determined in duplicate. The results are expressed as the percentage of maximal stimulation caused by a maximal effective concentration of peptide-1 (1 μM) without Bantag-1 present. The maximal stimulated [^{3}H]IP value for 1 μM peptide-1 (A) was 93,650 ± 3640 dpm, and the control value was 6620 ± 980 dpm (n = 6); with 1 μM MK-5046 (B), the maximal was 74,600 ± 2310 dpm and the control value was 3017 ± 860 dpm (n = 6). Inserts show the Schild plots calculated by least-squares curve fitting for peptide-1 and for MK-5046 from the average of at least three experiments.

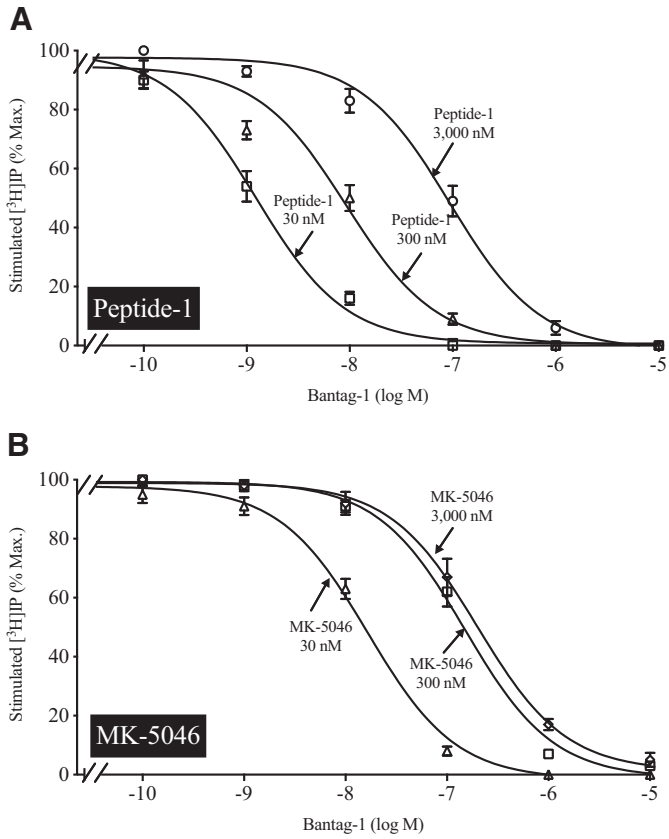

Fig. 4. Effect on the dose-inhibition curves of the BRS-3 antagonist Bantag-1 on [^{3}H]IP generation in hBRS-3/BALB with increasing concentrations of the peptide BRS-3 agonist peptide-1 (A) or the nonpeptide agonist MK-5046 (B). After loading the cells with 3 μCi/ml myo-[2-^{3}H]inositol, cells were incubated with each peptide at the indicated concentration for 60 minutes at 37°C. The [^{3}H]IP measurement was determined as described in *Materials and Methods*. The results are the mean and S.E.M. from at least three separate experiments, and in each experiment the data points were determined in duplicate. The results are expressed as the percentage of stimulation caused by the maximal effective concentration of peptide-1 (1 μM) or MK-5046 (3 μM) alone. The maximal stimulated [^{3}H]IP value by 1 μM peptide-1 was 85,600 ± 3720 dpm, and the control value was 9850 ± 1540 dpm (n = 5); for 1 μM MK-5046, the maximal stimulation of [^{3}H]IP was 66,930 ± 2370 dpm and the control value was 6490 ± 980 dpm (n = 5).

inhibition (Fig. 3) (Schild, 1997; Kenakin, 1982). Analysis of the data in Fig. 3A yielded an equilibrium coefficient of 1.84 ± 0.08 nM for Bantag-1.

A similar result was seen when the experiment was performed in the reverse manner, assessing the effects with increasing concentrations of each agonist on their Bantag-1 dose-inhibition curves for stimulation of IP generation (Fig. 4). In hBRS-3/BALB cells, increasing concentrations of Bantag-1 progressively inhibited 30 nM peptide-1 (Fig. 4A) and 30 nM MK-5046 (Fig. 4B) stimulation of phosphoinositide generation. With increasing concentrations of peptide-1 (300 and 3000 nM) there was a progressive proportional rightward shift in the Bantag-1 dose-inhibition curves (IC_{50}s: 1.2, 9.2, and 94 nM Bantag-1 with 30, 300, and 3000 nM peptide-1; Fig. 4A). However, this was not the case with MK-5046 (Fig. 4B). With increasing concentrations of MK-5046 (300 and 3000 nM), there was not a progressive proportional rightward shift of the Bantag-1 dose-inhibition curves, and in fact there was no difference seen in the IC_{50}s of Bantag-1 with 300- or 3000-nM MK-5046 concentrations (IC_{50}s: 17, 150, and 199 nM for Bantag-1; 30, 300, and 3000 nM MK-5046; Fig. 4B). These results demonstrated a decreasing effectiveness of the nonpeptide agonist MK-5046 at high concentrations in competing with the BRS-3 competitive antagonist Bantag-1, which is characteristic of the saturable effect reported with allosteric modulators (Christopoulos, 2002; Christopoulos and Kenakin, 2002; Fasciani et al., 2020). These results further support the conclusion that Bantag-1 is functioning as a competitive antagonist for the peptide-1 binding sites mediating PLC activation; however, it is functioning in a noncompetitive manner for the MK-5046 binding sites mediating PLC activation, suggesting that MK-5046 may be acting at a different site than peptide-1 to activate the BRS-3 receptor (i.e., in an allosteric manner).

The presence of allosteric modulation can be further supported by demonstrating an inability of an antagonist to shift the agonist dose-response curve with increasing agonist concentration, which can be manifested as a curvilinear Schild

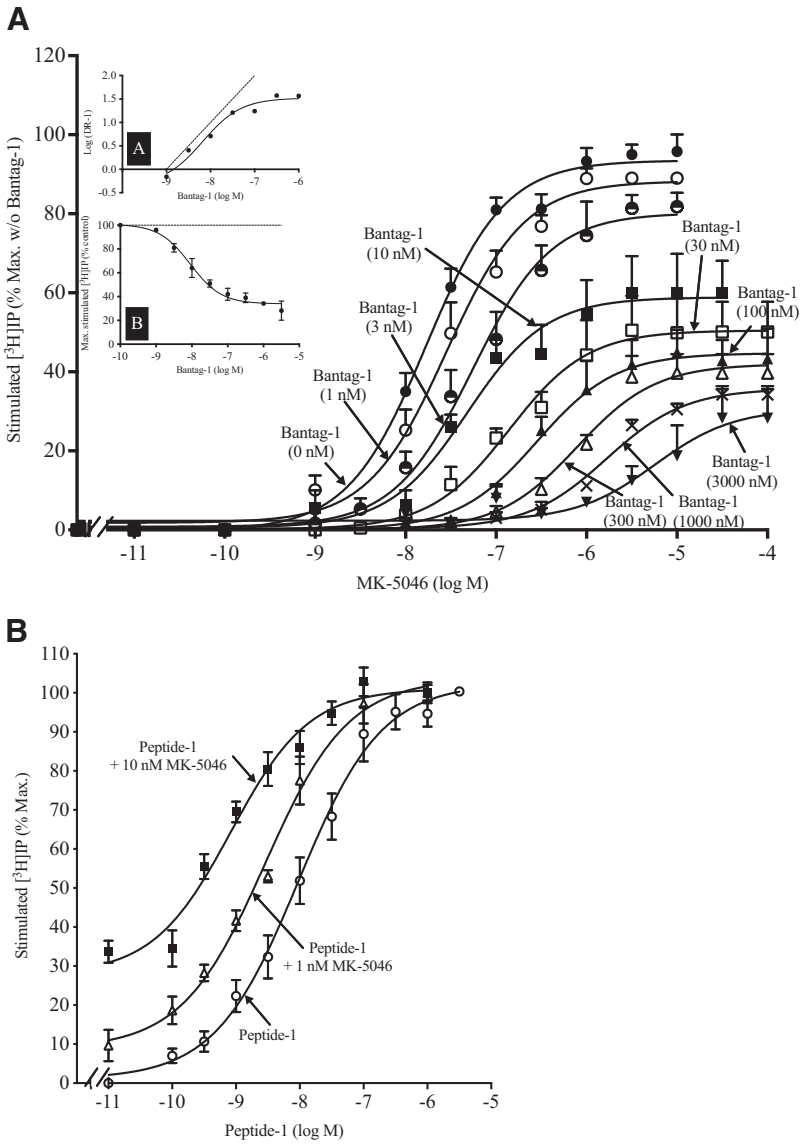

Fig. 5. Comparison of the ability of low and high concentrations of Bantag-1 (1 nM-3 μM), a BRS-3 receptor competitive antagonist, to alter the dose-responses of the nonpeptide agonist MK-5046 for stimulation of [^{3}H]IP generation in hBRS-3/BALB cells (A) and the ability of MK-5046 to affect the dose response curve for peptide -1 in these cells (B). After loading the cells with 3 μCi/ml myo-[2-^{3} H]inositol by incubating overnight, cells were then washed and incubated with each agonist (MK-5046, peptide-1) or antagonist (Bantag-1) at the indicated concentrations for 60 minutes at 37°C. The [^{3}H]IP measurement was determined as described in *Materials and Methods*. The results are the mean and S.E.M. from at least six separate experiments, and in each experiment the data points were determined in duplicate. The results are expressed as the percentage of maximal stimulation caused by the maximal effective concentration MK-5046 (1 μM) without Bantag-1 present (A) or Bantag-1 alone (B). The maximal stimulated [^{3}H]IP values were similar to those listed in the Fig. 3 legend. Inserts in the top panel show the Schild plot for the effect on MK-5046 potency at different Bantag-1 concentrations (insert A) and the effect on the efficacy (maximal stimulation) of MK-5046 with increasing Bantag-1 concentrations (insert B), each determined by a least-squares curve fitting analysis, which is the average of at least five experiments. The dotted line shows the expected results with an orthosteric agonist.

plot with a competitive antagonist (Eglen et al., 1988; Tränkle et al., 1998a; Langmead et al., 2006; Lanzafame et al., 2006). To study the reduction of efficacy observed with MK-5046 in more detail, we studied the dose-response effect on IP generation of the nonpeptide agonist MK-5046 with increasing high concentrations of the BRS-3 competitive antagonist Bantag-1 (Fig. 5, top). Although there was also a progressive rightward shift of the MK-5046 dose-response curve with these higher concentrations of Bantag-1, the extent of shift decreased and stopped when Bantag-1 concentrations of up to 1000 nM were used, when the MK-5046's EC_{50}s were not different (800 and 759 nM, respectively), and when 300 and 1000 nM Bantag-1 were present (Fig. 5, top). These data support the conclusion that MK-5046 was functioning in a noncompetitive allosteric manner at the binding sites responsible for cell activation. A Schild plot (Fig. 5A, insert A) of the inhibitory effect of Bantag-1 supports this conclusion by showing a linear correlation with a slope of 0.88 ± 0.06, which was not significantly different from unity, with the regression equation for low concentrations of Bantag-1 (i.e., 3 nM, 10 nM, and 30 nM); however, with higher concentrations of Bantag-1 (i.e., ≥30 nM), the regression curve demonstrated a curvilinear pattern with the slope increasingly differing from unity, yielding an overall slope of 0.56 ± 0.16 (Fig. 5A, insert A; $P < 0.0006$) consistent with noncompetitive,

allosteric behavior (Fig. 5A, insert A). To analyze the relationship between the effect of increasing concentrations of Bantag-1 on the efficacy of MK-5046, the relationship of the efficacy of MK-5046 at each Bantag-1 concentration was analyzed by a least-squares curve-fitting program (Fig. 5A, insert B). Similar to the effect of high concentrations of Bantag-1 on MK-5046 affinity revealed by the plateauing effect seen on the Schild plot (Fig. 5A, insert), at higher concentrations of Bantag-1 there was a plateauing effect of higher Bantag-1 concentrations on MK-5046 efficacy (Fig. 5A, insert B).

Effect of Various Concentrations of Nonpeptide Agonist MK-5046 To Affect the Dose-Response Curves for Activation of PLC and Generation of [^{3}H]IP by the Orthosteric Agonist Peptide-1

One of the frequently used methods to directly detect allosteric receptor interaction is to assess the effect of a putative allosteric agonist and an orthosteric agonist on their dose-response curves for receptor activation (Holst et al., 2005; Lee et al., 2008; Desai et al., 2019).When either of two submaximal concentrations of MK-5046 (i.e., 1 and 10 nM), which caused a respective 10% and 30% maximal activation when present alone (Fig. 5B), were added, thus increasing concentrations of peptide-1 for stimulating increasing generation of [^{3}H]IP, the dose-response curve for peptide-1 was potentiated with a 3-fold leftward shift with peptide-1 plus 1 nM MK-5046 and a 9-fold leftward shift with peptide-1 plus 10 nM MK-5046, supporting an allosteric effect of MK-5046.

Assessment of the Effect of MK-5046 on the Dissociation Binding Rate of the Specific BRS-3 Ligand ^{125}I-Bantag-1 from Plasma Membranes of hBRS-3/BALB Cells

Another frequently used method to directly detect allosteric receptor interaction is to assess ligand dissociation rates in the presence or absence of the proposed allosteric modulator (Kostenis and Mohr, 1996; Christopoulos and Kenakin, 2002; May and Christopoulos, 2003; May et al., 2004; Langmead et al., 2006; Langmead and Christopoulos, 2006). To assess the possible effect of the presence of MK-5046 on BRS-3 ligand dissociation rate, we assessed its effect on the dissociation of ^{125}I-Bantag-1 after allowing equilibrium binding to plasma membranes from hBRS-3/BALB cells (Fig. 6). The dissociation rate was 1.67-fold slower when MK-5046 was added (Fig. 6). Specifically, ^{125}I-Bantag-1 rapidly dissociated, and after 5 minutes the specific binding without MK-50461 was already 72% dissociated; whereas if MK-5046 was added at zero time, MK-5046 was only 55% ($P < 0.05$). Overall, the addition of MK-5046 resulted in a slowing of the dissociation rate to 0.324 ± 0.040/min from 0.194 ± 0.009/min without MK-5046 present ($P = 0.0053$) (Fig. 6). This result provides strong support for MK-5046 functioning as an allosteric modulator at the hBRS-3 receptor in these membranes (Kostenis and Mohr, 1996; Christopoulos and Kenakin, 2002; May and Christopoulos, 2003; May et al., 2004; Langmead et al., 2006; Langmead and Christopoulos, 2006).

Ability of Bantag-1, MK-5046, and Peptide-1 To Inhibit Binding of the ^{125}I-Bantag-1 at 50 pM and 3 nM to hBRS-3/BALB Cells

Another direct binding method frequently used to detect the presence of an allosteric modulator is to use different

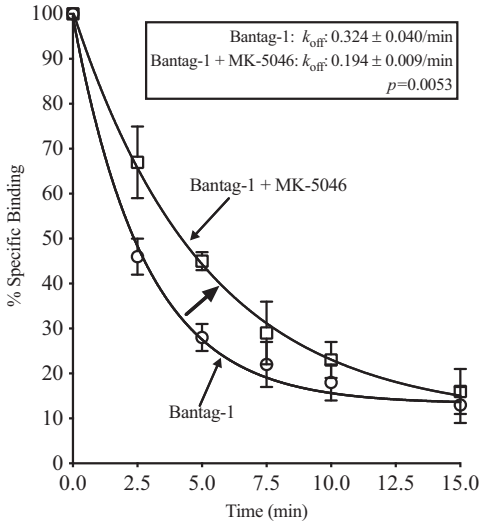

Fig. 6. Effect of MK-5046 on the dissociation of the radiolabeled antagonist ^{125}I-Bantag-1 from hBRS-3/BALB cell membranes (1×10^7 cells membranes/ml). hBRS-3/BALB membranes were incubated with 50 pM ^{125}I-Bantag-1 for 60 minutes at 22°C and were then incubated with or without 0.1 μM Bantag-1 or 0.1 μM Bantag-1 plus 1 μM MK-5046 for the indicated times. Results are expressed as the percentage of saturable binding with no additions. The results are the mean and S.E.M. from at least three separate experiments, and in each experiment the data points were determined in duplicate. The arrow shows the direction of the effect of the addition of MK-5046 on the dissociation of ^{125}I-Bantag-1.

concentrations of an orthosteric radioligand in binding assays because the saturating effect of the allosteric modulator becomes more evident as the concentration of the orthosteric radioligand is increased (Christopoulos and Kenakin, 2002; May and Christopoulos, 2003; May et al., 2004; Langmead et al., 2006; Langmead and Christopoulos, 2006). Therefore, the effects of different concentrations of the specific BRS-3 ligand ^{125}I-Bantag-1 on the binding of peptide-1 and the competitive BRS-3 specific ligand Bantag-1 were compared with that of MK-5046 (Fig. 7). We performed such a study by comparing the effect of a 60-fold difference in concentration (50 pM vs. 3 nM) of the orthosteric radioligand ^{125}I-Bantag-1 on the dose-inhibition curves ability of the nonpeptide agonist MK-5046 to those of the peptide antagonist Bantag-1 and the peptide agonist peptide-1 to inhibit binding of ^{125}I-Bantag-1 (Fig. 7). With both concentrations of ^{125}I-Bantag-1, the unlabeled BRS-3 peptide antagonist Bantag-1 (Fig. 7A) and the peptide agonist peptide-1 (Fig. 7C) caused a dose-dependent inhibition, with maximal inhibition to the same degree with both radioligand concentrations, when sufficiently high concentrations of the unlabeled peptides were added (Fig. 7, A and C). However, this was not the case with MK-5046 (Fig. 7B), in which the inhibitory effect of high concentrations of the unlabeled nonpeptide agonist MK-5046 was much less effective with the high concentration of radioligand (Fig. 7B). Specifically, maximal concentrations of MK-5046 inhibited maximal binding of 50 pM ^{125}I-Bantag-1 by 40%; but with 3 nM ^{125}I-Bantag-1, maximal effect concentrations of MK-5046 only inhibited binding by 7% (a 5.7-fold reduction) (Fig. 7B). This difference in efficacy of inhibition with the two radioligand concentrations occurred without any change in the MK-5046 inhibitory potency with the

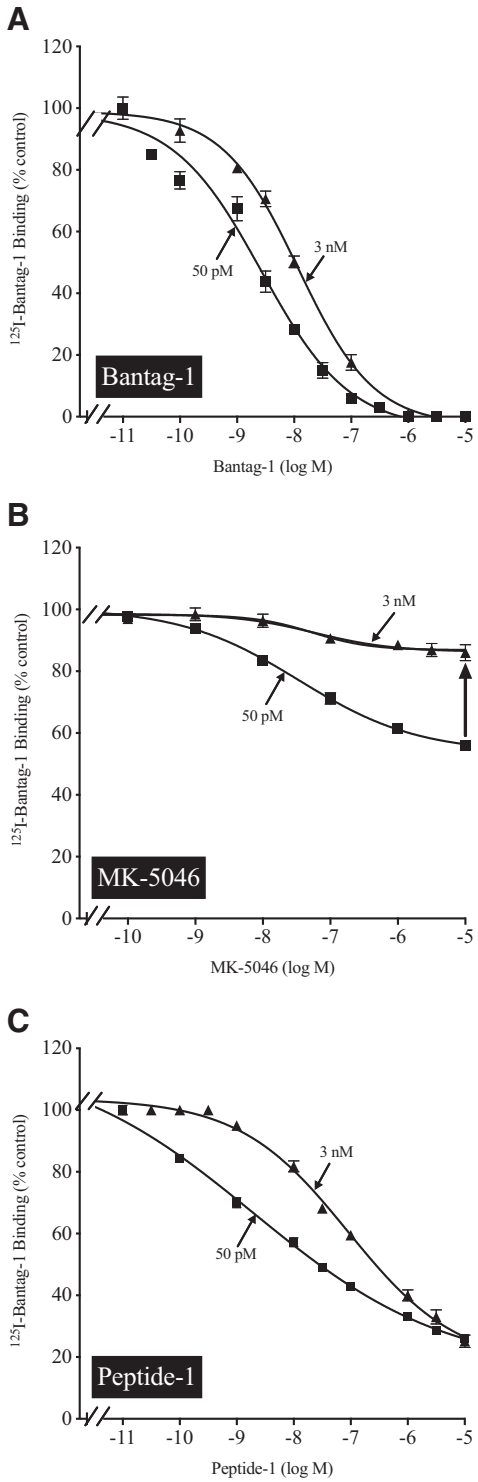

Fig. 7. Effect of different concentrations of the radioligand ^{125}I-Bantag-1 (50 pM, 3 nM) on the dose-inhibition curves of unlabeled Bantag-1, MK-5046, or peptide-1 for inhibiting the binding to hBRS-3/BALB cells. hBRS-3/BALB cells (1×10^6 cells/ml) were incubated with 50 pM or 3 nM ^{125}I-Bantag-1, with or without increasing concentrations of Bantag-1, MK-5046, or peptide-1 for 60 minutes at 22°C. Results are expressed as the percentage of saturable binding with no additions. The results are the mean and S.E.M. from at least three separate experiments, and in each experiment the data points were determined in duplicate. The arrow in (B) shows the marked effect of the different ligand concentrations on the maximal suppression of the radioligand binding with MK-5046 (10 μM) compared with the lack of effect and complete inhibition seen with a high concentration of Bantag-1 (1 μM) (A) or peptide-1 (10 μM) (C).

two different radioligand concentrations (i.e., IC_{50}: 53 ± 3 vs. 42 ± 2 nM), which is characteristic for an allosteric modulator (Christopoulos and Kenakin, 2002; May and Christopoulos, 2003; May et al., 2004; Langmead et al., 2006; Langmead and Christopoulos, 2006).

Comparison of Receptor Domains Responsible for Affinity of Bantag-1 or MK-5046 in hBRS-3 Using Receptor Chimeras and Site-Directed Mutagenesis

Allosteric modulators are receptor ligands that interact with binding sites that are topographically distinct from the characteristic orthosteric binding site (May et al., 2004, 2007; Wootten et al., 2017). The above data support the conclusion that the nonpeptide agonist MK-5046 and the peptide agonist peptide-1 bind to different sites to activate BRS-3, which could be distinguished by the competitive BRS-3 antagonist Bantag-1. Although the native ligand of BRS-3 is unknown, the pan-hBnR synthetic agonist peptide-1 has been shown to interact with the orthosteric binding sites in the same manner as the native ligands (Pradhan et al., 1998) in all of the BnRs studied, including hGRPRs/hNMBRs, GRPRs and NMBRs from a number of other species, and the nonmammalian BB4 receptor, supporting the conclusion that it is acting at the orthosteric binding site of these BnRs. To provide additional direct support for the above conclusion that MK-5046 is acting at an allosteric site, a chimeric receptor approach as well as a specific BRS-3 point mutation were studied. In previous studies, MK-5046 and Bantag-1 have been shown to have a high selectivity for BRS-3 over GRPR or NMBR (Guan et al., 2010; Moreno et al., 2013; Ramos-Álvarez et al., 2015; Nakamura et al., 2016) in contrast to peptide-1, which is not selective for BRS-3 and instead has a high affinity for both hBRS-3 and GRPR (Pradhan et al., 1998; González et al., 2009; Ramos-Álvarez et al., 2015; Nakamura et al., 2016). As reported previously (Guan et al., 2010; Moreno et al., 2013; Ramos-Álvarez et al., 2015; Nakamura et al., 2016), we found that GRPR had low affinity for both Bantag-1 and MK-5046 (>30,000 nM), whereas each had high affinity for BRS-3 (Table 2). We took advantage of these marked differences in affinity of Bantag-1, MK-5046, and peptide-1 for BRS-3 and GRPR to provide possible insight into their different binding domains in BRS-3 by making MK-5046 and Bantag-1 gain-of-affinity GRPR chimeras. This was accomplished by the substitution of each extracellular loop of BRS-3 (i.e., EC1, EC2, and EC3), which has high affinity for MK-5046 and Bantag-1, into GRPR, which has low affinity for each of these ligands (Table 2). The substitution of extracellular loop 1 of BRS-3 for that of GRPR [(ec1-BRS-3) GRPR] markedly increased affinity for Bantag-1 (i.e., increased affinity from >30,000 nM to 6700 nM) but had no effect on the affinity of MK-5046 (Table 2). In contrast, the substitution of the second extracellular loop of BRS-3 (ec2-BRS-3) into GRPR [(ec2-BRS-3) GRPR] markedly increased the affinity of MK-5046 (i.e., from >30,000 nM to 7573 nM) but had no effect on this affinity of Bantag-1 (Table 2). The substitution of third extracellular loop of BRS-3 for EC3 of GRPR [(ec3-BRS-3) GRPR] had no effect on affinity of either ligand (Table 2). These data demonstrate that the binding sites determining high affinity for these two ligands markedly differ. A previous study (Nakamura et al., 2016) reported that Arg^{127} in the third transmembrane region of BRS-3 was critical for high affinity with Bantag-1. To explore

TABLE 2
Affinities of Bantag-1 and MK-5046 for wild-type BRS-3/GRPR, BRS-3$^{\Delta}$ (BRS-3 loss of affinity), and extracellular chimeric BRS-3/GRPRs (GRPR gain of affinity)
CHOP cells were transiently transfected with lipofectamine as described previously (Nakamura et al., 2016) and incubated with 50 pM ^{125}I-peptide-1 for 60 min at 21°C, and binding was determined as described in *Materials and Methods*. In each experiment, each value was determined in duplicate and values given are mean and S.E.M. from at least three separate experiments. Data are calculated from dose-inhibition curves using a nonlinear regression curve-fitting program (Prism).

		IC_{50} (nM)	
	Location	Bantag-1	MK-5046
BRS-3		5.6 ± 0.4[a]	137 ± 30
GRPR		>30,000[a]	>30,000
Extracellular Chimeras (GRPR Gain of Affinity)		[vs. Wild-Type GRPR]	
(ec1-BRS-3) GRPR		6700 ± 440[a,b]	>30,000
(ec2-BRS-3) GRPR		>30,000[a]	7573 ± 548[b]
(ec3-BRS-3) GRPR		>30,000[a]	27,726 ± 2274
BRS-3 Point Mutation (Loss of Affinity)		[vs. Wild-Type BRS-3]	
BRS-3$^{\Delta c}$ [R127Q BRS-3]	3.32	1332 ± 182[a,d]	86 ± 7.2[d]

[a]Data from (Nakamura et al., 2016).
[b]$P < 0.05$ compared with wild-type GRPR.
[c]In BRS-3$^{\Delta}$, Arg^{127} in native BRS-3 is substituted for by Gln, which is in a comparable position of GRPR.
[d]$P < 0.05$ compared with wild-type BRS-3.

whether this was also true with MK-5046, a possible loss-of-affinity point mutation in BRS-3 was made by replacing Arg^{127} in BRS-3 with glutamine, which exists in a similar position in the GRPR, which has low affinity for Bantag-1 (Ramos-Álvarez et al., 2015; Nakamura et al., 2016). The substitution of arginine by glutamine in position 127 of BRS-3 in the third transmembrane domain decreased the affinity for Bantag-1 by 236-fold (IC_{50}: 5.6 to 1332 nM; Table 2), whereas it had no effect on the affinity of MK-5046 (Table 2). These data demonstrate that the molecular determinants of high-affinity receptor interaction of these two agonist ligands differ markedly, suggesting marked differences in their high-affinity receptor binding pockets.

Discussion

A number of the findings in this study support the conclusion that the BRS-3 receptor nonpeptide agonist MK-5046 is functioning as allosteric agonist. First, binding studies using ^{125}I-Bantag-1, a recently described high-affinity, specific peptide antagonist BRS-3 ligand (Ramos-Alvarez et al., 2019), demonstrated that MK-5046 only partially inhibited (i.e., <50%) the total saturable binding to BRS-3 transfected cells and 417 lung cancer cells possessing native BRS-3 receptors (Ryan et al., 1998b; Sancho et al., 2010; Moreno et al., 2013). In contrast, the orthosteric agonist peptide-1 (Mantey et al., 1997) and the BRS-3 antagonists Bantag-1 and D-PT-SP (Mantey et al., 1997; Guan et al., 2010; Moreno et al., 2013) inhibited the saturable binding by >90% to 100%. These results show that MK-5046 does not fully interact with the majority of the orthosteric sites and may be acting allosterically, a pattern reported with a number of other allosteric ligands (Tränkle et al., 1998a; Langmead and Christopoulos, 2006). This incomplete inhibition of the binding of the orthosteric ligand by MK-5046 fulfills one of the proposed criteria required for confirming allosteric drug interaction (Langmead and Christopoulos, 2006). Second, this possibility was strongly supported by the differing effects of the BRS-3 specific receptor-antagonist Bantag-1 on the ability of the orthosteric ligand peptide-1 and MK-5046 to activation/stimulation of phospholipase C, the principal signal cascade mediating BRS-3's actions (Jensen et al., 2008; Moreno et al., 2013; Alexander et al., 2019). Although Bantag-1 showed a competitive interaction with peptide-1, with MK-5046 the interaction was noncompetitive in its effect on efficacy and affinity. Furthermore, the Schild plot showed the typical linear pattern with a slope not differing from unity with increasing antagonist/agonist concentration with the orthosteric ligand peptide-1. In contrast, a curvilinear pattern with the Schild plot was seen with MK-5046, showing a decreasing effectiveness of MK-5046 at higher concentrations, suggesting a saturable effect or ceiling effect characteristically seen with allosteric ligands (Tränkle et al., 1998a; Christopoulos, 2002; Christopoulos and Kenakin, 2002; Langmead et al., 2006; Fasciani et al., 2020). Third, MK-5046 decreased the dissociation rate of the BRS-3 orthosteric radiolabeled antagonist ^{125}I-Bantag-1. The assessment of the effect of a ligand on dissociation of an allosteric ligand is one of the approaches generally recommended to detect allosteric interactions (Kostenis and Mohr, 1996; Christopoulos and Kenakin, 2002; May and Christopoulos, 2003; May et al., 2004; Langmead et al., 2006; Langmead and Christopoulos, 2006). This approach takes advantage of fact that the dissociation rate of a preequilibrated receptor-orthosteric radioligand complex can only be affected if that complex is altered in an allosteric manner (Kostenis and Mohr, 1996; Christopoulos, 2002; Christopoulos and Kenakin, 2002; May and Christopoulos, 2003; May et al., 2004; Langmead et al., 2006; Langmead and Christopoulos, 2006). Alterations can occur in the dissociation rate of the receptor-orthosteric radioligand complex if it is assessed under nonequilibrium conditions; however, that was not the case in our study because ^{125}I-Bantag-1 both binds and dissociates rapidly, reaching equilibrium by 10–15 minutes (Ramos-Alvarez et al., 2019) with our study performed after 60 minutes to ensure equilibrium. Fourth, we found that increasing the orthosteric ligand concentration had a marked effect on the dose-inhibition curve by MK-5046, which did not occur seen with the orthosteric ligands Bantag-1 or peptide-1. This result is characteristic of an allosteric interaction (Christopoulos and Kenakin, 2002; May and Christopoulos,

2003; May et al., 2004; Langmead et al., 2006; Langmead and Christopoulos, 2006). It takes advantage of the fact that an allosteric ligand demonstrates a saturating or ceiling effect that becomes more evident as the concentration of the orthosteric radioligand is increased (Christopoulos and Kenakin, 2002; May and Christopoulos, 2003; May et al., 2004; Langmead et al., 2006; Langmead and Christopoulos, 2006). Fifth, in a functional assay assessing activation of phospholipase C, MK-5046 leftward shifted the dose-response curve of the orthosteric agonist peptide-1, which is characteristic for an allosteric interaction (Holst et al., 2005; Lee et al., 2008; Desai et al., 2019). These results demonstrate that MK-5046 joins an increasing group of allosteric ligands for other GPCRs, which recently include those for muscarinic cholinergic receptors, dopamine, serotonin, various GI hormone/neurotransmitter receptors (i.e., cholecystokinin, GLP1, Glucagon, opioids, etc.), and several other GPCRs (Tränkle et al., 1998a,b; Christopoulos, 2002; Christopoulos and Kenakin, 2002; Langmead et al., 2006; Langmead and Christopoulos, 2006; May et al., 2007; Gao et al., 2008; Langmead and Christopoulos, 2014; Dong et al., 2015; Fasciani et al., 2020; Wootten and Miller, 2020; Mizera and Latek, 2021).

Unfortunately, there are only a few ligand binding studies that provide any information on the important amino acids determining the high affinity or selectivity of these three BRS-3 ligands (peptide-1, Bantag-1, and MK-5046) that can be looked to for any direct insight of possible different/similar receptor binding pockets. Some data from binding studies of the BRS-3 receptor structural sites identified by receptor chimera and receptor mutagenesis studies, which are important in determining high-affinity binding for BRS-3 of either peptide-1 (Uehara et al., 2012) or Bantag-1 (Nakamura et al., 2016), have been published; however, there are no studies in this area with MK-5046. Nevertheless, some results from these studies, as well as the limited molecular results from BRS-3 chimeras and BRS-3 mutagenesis included in the current study, support the results of the present study that peptide-1 and Bantag-1 interact at the same binding site whereas MK-5046 acts at a distinct allosteric site. Using ^{125}I-Peptide 1 as the ligand (Nakamura et al., 2016), Bantag-1 was found to bind with high affinity to hBRS-3 [inhibition constant (K_i) = 5.2 nM] and to have a >6000-fold selectivity for BRS-3 over GRPR/NMBR (Nakamura et al., 2016). When Bantag-1 binding was examined using the interactions of ^{125}I-Peptide 1 with BRS-3/GRPR chimeras (i.e., using Bantag-1 loss- and gain-of-affinity chimeras) and when site-directed mutagenesis was performed (Nakamura et al., 2016), it was found that interaction, particularly with the BRS-3 extracellular domains, was important for Bantag-1's high-affinity/selectivity interaction with relative importance of EC1≫EC2≫EC3 (EC1) (Nakamura et al., 2016) (Table 2) and that three amino acids within EC1 (H107, E111, and G112) were particularly important, as was the amino acid R127 in transmembrane region 3 (TM3). Another binding study (Uehara et al., 2012) reported that peptide-1's high affinity for BRS-3 as well as a number of other BnRs also required interaction with EC1 (i.e., particularly G112 and D97 within this domain), supporting the conclusion that these two ligands interact with similar receptor domains, as found in the present study. In contrast, results in the present study reveal that when studies of the binding interaction of MK-5046 with BRS-3/GRPR chimeras followed with site-directed mutagenesis were performed, different binding sites were involved in determining its high-affinity interaction. Specifically, these results showed that for MK-5046, EC2 but not EC1 (as was the case with Bantag-1/peptide-1) was the most important EC domain and that in TM3, R127 was not an important determinant of MK-5046 high affinity as it was for Bantag-1, supporting the conclusion that MK-5046 was binding at an allosteric site.

In conclusion, we consider that the most important finding in this study is the first identification of a ligand for the bombesin receptor family that acts allosterically. Despite many studies suggesting important roles for this receptor family in numerous physiologic processes as well as several important pathophysiological processes (especially feeding behavior, pruritis, numerous CNS disorders, regulation of insulin release, and glucose homeostasis), none of these studies have resulted in clinically useful therapeutic agents. This is in large part due to lack of highly specific drugs to explore these roles. For example, the use of BRS-3 agonists such as MK-5046 in satiety have been limited by side effects. Recently, with several other GPCRs/receptors in other systems/disorders, there has been very promising success with the use of allosteric agents with their enhanced specificity, biased signaling, ceiling effect, and probe dependence. Unfortunately, from the discovery of the first allosteric ligand to the eventual development of a therapeutic agent can take over 10 years, such as seen with allosteric ghrelin analogs now being considered for possible treatment of cachexia, for GI motility, or as anti-obesity agents (Holst et al., 2005). We hope that this description of MK-5046 functioning in an allosteric manner will lead to increased interest in this approach with this group of receptors.

Authorship Contributions

Participated in research design: Ramos-Alvarez, Iordanskaia, Mantey, Jensen.

Conducted experiments: Ramos-Alvarez, Iordanskaia, Mantey, Jensen.

Contributed new reagents or analytic tools: Ramos-Alvarez, Iordanskaia, Mantey, Jensen.

Performed data analysis: Ramos-Alvarez, Iordanskaia, Mantey, Jensen.

Wrote or contributed to the writing of the manuscript: Ramos-Alvarez, Iordanskaia, Mantey, Jensen.

References

Alexander SPH, Christopoulos A, Davenport AP, Kelly E, Mathie A, Peters JA, Veale EL, Armstrong JF, Faccenda E, Harding SD, et al.; CGTP Collaborators (2019) The Concise Guide to Pharmacology 2019/20: G protein-coupled receptors. *Br J Pharmacol* **176** (Suppl 1):S21–S141.

Arunlakshana O and Schild HO (1997) Some quantitative uses of drug antagonists. 1958. *Br J Pharmacol* **120** (Suppl 4):151–161, discussion 148–150.

Battey J, Benya RV, Jensen RT, and Moody TW (2021). Bombesin receptors in GtoPdb v.2021.2. *IUPHAR BPS Guide Pharm CITE* **2021** DOI: 10.2218/gtopdb/F9/2021.2.

Benya RV, Fathi Z, Battey JF, and Jensen RT (1993) Serines and threonines in the gastrin-releasing peptide receptor carboxyl terminus mediate internalization. *J Biol Chem* **268**:20285–20290.

Benya RV, Fathi Z, Kusui T, Pradhan T, Battey JF, and Jensen RT (1994) Gastrin-releasing peptide receptor-induced internalization, down-regulation, desensitization, and growth: possible role for cyclic AMP. *Mol Pharmacol* **46**:235–245.

Benya RV, Kusui T, Pradhan TK, Battey JF, and Jensen RT (1995) Expression and characterization of cloned human bombesin receptors. *Mol Pharmacol* **47**:10–20.

Benya RV, Wada E, Battey JF, Fathi Z, Wang LH, Mantey SA, Coy DH, and Jensen RT (1992) Neuromedin B receptors retain functional expression when transfected into BALB 3T3 fibroblasts: analysis of binding, kinetics, stoichiometry, modulation by guanine nucleotide-binding proteins, and signal transduction and comparison with natively expressed receptors. *Mol Pharmacol* **42**:1058–1068.

Cawston EE, Lam PC, Harikumar KG, Dong M, Ball AM, Augustine ML, Akgün E, Portoghese PS, Orry A, Abagyan R, et al. (2012) Molecular basis for binding and subtype selectivity of 1,4-benzodiazepine antagonist ligands of the cholecystokinin receptor. *J Biol Chem* **287**:18618–18635.

Christopoulos A (2002) Allosteric binding sites on cell-surface receptors: novel targets for drug discovery. *Nat Rev Drug Discov* **1**:198–210.

Christopoulos A (2014) Advances in G protein-coupled receptor allostery: from function to structure. *Mol Pharmacol* **86**:463–478.
Christopoulos A and Kenakin T (2002) G protein-coupled receptor allosterism and complexing. *Pharmacol Rev* **54**:323–374.
Coy DH, Taylor JE, Jiang NY, Kim SH, Wang LH, Huang SC, Moreau JP, Gardner JD, and Jensen RT (1989) Short-chain pseudopeptide bombesin receptor antagonists with enhanced binding affinities for pancreatic acinar and Swiss 3T3 cells display strong antimitotic activity. *J Biol Chem* **264**:14691–14697.
Desai AJ, Mechin I, Nagarajan K, Valant C, Wootten D, Lam PCH, Orry A, Abagyan R, Nair A, Sexton PM, et al. (2019) Molecular basis of action of a small-molecule positive allosteric modulator agonist at the type 1 cholecystokinin holoreceptor. *Mol Pharmacol* **95**:245–259.
Dong M, Vattelana AM, Lam PC, Orry AJ, Abagyan R, Christopoulos A, Sexton PM, Haines DR, and Miller LJ (2015) Development of a highly selective allosteric antagonist radioligand for the type 1 cholecystokinin receptor and elucidation of its molecular basis of binding. *Mol Pharmacol* **87**:130–140.
Eglen RM, Montgomery WW, Dainty IA, Dubuque LK, and Whiting RL (1988) The interaction of methoctramine and himbacine at atrial, smooth muscle and endothelial muscarinic receptors in vitro. *Br J Pharmacol* **95**:1031–1038.
Fasciani I, Petragnano F, Aloisi G, Marampon F, Carli M, Scarselli M, Maggio R, and Rossi M (2020) Allosteric modulators of G protein-coupled dopamine and serotonin receptors: a new class of atypical antipsychotics. *Pharmaceuticals (Basel)* **13**:388.
Feng Y, Guan XM, Li J, Metzger JM, Zhu Y, Juhl K, Zhang BB, Thornberry NA, Reitman ML, and Zhou YP (2011) Bombesin receptor subtype-3 (BRS-3) regulates glucose-stimulated insulin secretion in pancreatic islets across multiple species. *Endocrinology* **152**:4106–4115.
Gao F, Sexton PM, Christopoulos A, and Miller LJ (2008) Benzodiazepine ligands can act as allosteric modulators of the type 1 cholecystokinin receptor. *Bioorg Med Chem Lett* **18**:4401–4404.
Gonzalez N, Hocart SJ, Portal-Nuñez S, Mantey SA, Nakagawa T, Zudaire E, Coy DH, and Jensen RT (2008a) Molecular basis for agonist selectivity and activation of the orphan bombesin receptor subtype 3 receptor. *J Pharmacol Exp Ther* **324**:463–474.
González N, Mantey SA, Pradhan TK, Sancho V, Moody TW, Coy DH, and Jensen RT (2009) Characterization of putative GRP- and NMB-receptor antagonist's interaction with human receptors. *Peptides* **30**:1473–1486.
Gonzalez N, Moody TW, Igarashi H, Ito T, and Jensen RT (2008b) Bombesin-related peptides and their receptors: recent advances in their role in physiology and disease states. *Curr Opin Endocrinol Diabetes Obes* **15**:58–64.
González N, Moreno P, and Jensen RT (2015) Bombesin receptor subtype 3 as a potential target for obesity and diabetes. *Expert Opin Ther Targets* **19**:1153–1170.
Guan XM, Chen H, Dobbelaar PH, Dong Y, Fong TM, Gagen K, Gorski J, He S, Howard AD, Jian T, et al. (2010) Regulation of energy homeostasis by bombesin receptor subtype-3: selective receptor agonists for the treatment of obesity. *Cell Metab* **11**:101–112.
Guan XM, Metzger JM, Yang L, Raustad KA, Wang SP, Spann SK, Kosinski JA, Yu H, Shearman LP, Faidley TD, et al. (2011) Antiobesity effect of MK-5046, a novel bombesin receptor subtype-3 agonist. *J Pharmacol Exp Ther* **336**:356–364.
Heinz-Erian P, Coy DH, Tamura M, Jones SW, Gardner JD, and Jensen RT (1987) [D-Phe12]bombesin analogues: a new class of bombesin receptor antagonists. *Am J Physiol* **252**:G439–G442.
Holst B, Brandt E, Bach A, Heding A, and Schwartz TW (2005) Nonpeptide and peptide growth hormone secretagogues act both as ghrelin receptor agonist and as positive or negative allosteric modulators of ghrelin signaling. *Mol Endocrinol* **19**:2400–2411.
Jensen RT, Battey JF, Spindel ER, and Benya RV (2008) International Union of Pharmacology. LXVIII. Mammalian bombesin receptors: nomenclature, distribution, pharmacology, signaling, and functions in normal and disease states. *Pharmacol Rev* **60**:1–42.
Kenakin TP (1982) The Schild regression in the process of receptor classification. *Can J Physiol Pharmacol* **60**:249–265.
Khoury E, Clément S, and Laporte SA (2014) Allosteric and biased g protein-coupled receptor signaling regulation: potentials for new therapeutics. *Front Endocrinol (Lausanne)* **5**:68.
Kostenis E and Mohr K (1996) Two-point kinetic experiments to quantify allosteric effects on radioligand dissociation. *Trends Pharmacol Sci* **17**:280–283.
Langmead CJ and Christopoulos A (2006) Allosteric agonists of 7TM receptors: expanding the pharmacological toolbox. *Trends Pharmacol Sci* **27**:475–481.
Langmead CJ and Christopoulos A (2014) Functional and structural perspectives on allosteric modulation of GPCRs. *Curr Opin Cell Biol* **27**:94–101.
Langmead CJ, Fry VA, Forbes IT, Branch CL, Christopoulos A, Wood MD, and Herdon HJ (2006) Probing the molecular mechanism of interaction between 4-n-butyl-1-[4-(2-methylphenyl)-4-oxo-1-butyl]-piperidine (AC-42) and the muscarinic M(1) receptor: direct pharmacological evidence that AC-42 is an allosteric agonist. *Mol Pharmacol* **69**:236–246.
Lanzafame AA, Sexton PM, and Christopoulos A (2006) Interaction studies of multiple binding sites on m4 muscarinic acetylcholine receptors. *Mol Pharmacol* **70**:736–746.
Lee T, Schwandner R, Swaminath G, Weiszmann J, Cardozo M, Greenberg J, Jaeckel P, Ge H, Wang Y, Jiao X, et al. (2008) Identification and functional characterization of allosteric agonists for the G protein-coupled receptor FFA2. *Mol Pharmacol* **74**:1599–1609.
Li M, Liang P, Liu D, Yuan F, Chen GC, Zhang L, Liu Y, and Liu H (2019) Bombesin receptor subtype-3 in human diseases. *Arch Med Res* **50**:463–467.
Majumdar ID and Weber HC (2012a) Appetite-modifying effects of bombesin receptor subtype-3 agonists. *Handb Exp Pharmacol* **209**:405–432.
Majumdar ID and Weber HC (2012b) Biology and pharmacology of bombesin receptor subtype-3. *Curr Opin Endocrinol Diabetes Obes* **19**:3–7.
Mantey S, Frucht H, Coy DH, and Jensen RT (1993) Characterization of bombesin receptors using a novel, potent, radiolabeled antagonist that distinguishes bombesin receptor subtypes. *Mol Pharmacol* **43**:762–774.
Mantey SA, Weber HC, Sainz E, Akeson M, Ryan RR, Pradhan TK, Searles RP, Spindel ER, Battey JF, Coy DH, et al. (1997) Discovery of a high affinity radioligand for the human orphan receptor, bombesin receptor subtype 3, which demonstrates that it has a unique pharmacology compared with other mammalian bombesin receptors. *J Biol Chem* **272**:26062–26071.
Markussen J, Havelund S, Kurtzhals P, Andersen AS, Halstrøm J, Hasselager E, Larsen UD, Ribel U, Schäffer L, Vad K, et al. (1996) Soluble, fatty acid acylated insulins bind to albumin and show protracted action in pigs. *Diabetologia* **39**:281–288.
Matsufuji T, Shimada K, Kobayashi S, Ichikawa M, Kawamura A, Fujimoto T, Arita T, Hara T, Konishi M, Abe-Ohya R, et al. (2015) Synthesis and biological evaluation of novel chiral diazepine derivatives as bombesin receptor subtype-3 (BRS-3) agonists incorporating an antedrug approach. *Bioorg Med Chem* **23**:89–104.
Matsufuji T, Shimada K, Kobayashi S, Kawamura A, Fujimoto T, Arita T, Hara T, Konishi M, Abe-Ohya R, Izumi M, et al. (2014) Discovery of novel chiral diazepines as bombesin receptor subtype-3 (BRS-3) agonists with low brain penetration. *Bioorg Med Chem Lett* **24**:750–755.
May LT, Avlani VA, Sexton PM, and Christopoulos A (2004) Allosteric modulation of G protein-coupled receptors. *Curr Pharm Des* **10**:2003–2013.
May LT and Christopoulos A (2003) Allosteric modulators of G-protein-coupled receptors. *Curr Opin Pharmacol* **3**:551–556.
May LT, Leach K, Sexton PM, and Christopoulos A (2007) Allosteric modulation of G protein-coupled receptors. *Annu Rev Pharmacol Toxicol* **47**:1–51.
Mizera M and Latek D (2021) Ligand-receptor interactions and machine learning in GCGR and GLP-1R drug discovery. *Int J Mol Sci* **22**:4060.
Moody TW, Lee L, Ramos-Alvarez I, Iordanskaia T, Mantey SA, and Jensen RT (2021) Bombesin receptor family activation and CNS/neural tumors: review of evidence supporting possible role for novel targeted therapy. *Front Endocrinol (Lausanne)* **12**:728088.
Moody TW, Ramos-Alvarez I, and Jensen RT (2018) Neuropeptide G protein-coupled receptors as oncotargets. *Front Endocrinol (Lausanne)* **9**:345.
Moreno P, Mantey SA, Lee SH, Ramos-Álvarez I, Moody TW, and Jensen RT (2018) A possible new target in lung-cancer cells: the orphan receptor, bombesin receptor subtype-3. *Peptides* **101**:213–226.
Moreno P, Mantey SA, Nuche-Berenguer B, Reitman ML, González N, Coy DH, and Jensen RT (2013) Comparative pharmacology of bombesin receptor subtype-3, nonpeptide agonist MK-5046, a universal peptide agonist, and peptide antagonist Bantag-1 for human bombesin receptors. *J Pharmacol Exp Ther* **347**:100–116.
Moreno P, Ramos-Álvarez I, Moody TW, and Jensen RT (2016) Bombesin related peptides/receptors and their promising therapeutic roles in cancer imaging, targeting and treatment. *Expert Opin Ther Targets* **20**:1055–1073.
Nakamura T, Ramos-Álvarez I, Iordanskaia T, Moreno P, Mantey SA, and Jensen RT (2016) Molecular basis for high affinity and selectivity of peptide antagonist, Bantag-1, for the orphan BB3 receptor. *Biochem Pharmacol* **115**:64–76.
Nickols HH and Conn PJ (2014) Development of allosteric modulators of GPCRs for treatment of CNS disorders. *Neurobiol Dis* **61**:55–71.
Ohki-Hamazaki H, Watase K, Yamamoto K, Ogura H, Yamano M, Yamada K, Maeno H, Imaki J, Kikuyama S, Wada E, et al. (1997) Mice lacking bombesin receptor subtype-3 develop metabolic defects and obesity. *Nature* **390**:165–169.
Pradhan TK, Katsuno T, Taylor JE, Kim SH, Ryan RR, Mantey SA, Donohue PJ, Weber HC, Sainz E, Battey JF, et al. (1998) Identification of a unique ligand which has high affinity for all four bombesin receptor subtypes. *Eur J Pharmacol* **343**:275–287.
Qin X and Qu X (2021) Recent advances in the biology of bombesin-like peptides and their receptors. *Curr Opin Endocrinol Diabetes Obes* **28**:232–237.
Qu X, Wang H, and Liu R (2018) Recent insights into biological functions of mammalian bombesin-like peptides and their receptors. *Curr Opin Endocrinol Diabetes Obes* **25**:36–41.
Ramos-Alvarez I, Lee L, Mantey SA, and Jensen RT (2019) Development and characterization of a novel, high-affinity, specific, radiolabeled ligand for BRS-3 receptors. *J Pharmacol Exp Ther* **369**:454–465.
Ramos-Álvarez I, Moreno P, Mantey SA, Nakamura T, Nuche-Berenguer B, Moody TW, Coy DH, and Jensen RT (2015) Insights into bombesin receptors and ligands: highlighting recent advances. *Peptides* **72**:128–144.
Ramos-Alvarez I, Nakamura T, Mantey SA, Moreno P, Nuche-Berenguer B, and Jensen RT (2016) Novel chiral-diazepines function as specific, selective receptor agonists with variable coupling and species variability in human, mouse and rat BRS-3 receptor cells. *Peptides* **75**:8–17.
Reitman ML, Dishy V, Moreau A, Denney WS, Liu C, Kraft WK, Mejia AV, Matson MA, Stoch SA, Wagner JA, et al. (2012) Pharmacokinetics and pharmacodynamics of MK-5046, a bombesin receptor subtype-3 (BRS-3) agonist, in healthy patients. *J Clin Pharmacol* **52**:1306–1316.
Roesler R and Schwartsmann G (2012) Gastrin-releasing peptide receptors in the central nervous system: role in brain function and as a drug target. *Front Endocrinol (Lausanne)* **3**:159.
Rowley WH, Sato S, Huang SC, Collado-Escobar DM, Beaven MA, Wang LH, Martinez J, Gardner JD, and Jensen RT (1990) Cholecystokinin-induced formation of inositol phosphates in pancreatic acini. *Am J Physiol* **259**:G655–G665.
Ryan RR, Weber HC, Hou W, Sainz E, Mantey SA, Battey JF, Coy DH, and Jensen RT (1998a) Ability of various bombesin receptor agonists and antagonists to alter intracellular signaling of the human orphan receptor BRS-3. *J Biol Chem* **273**:13613–13624.
Ryan RR, Weber HC, Mantey SA, Hou W, Hilburger ME, Pradhan TK, Coy DH, and Jensen RT (1998b) Pharmacology and intracellular signaling mechanisms of the native human orphan receptor BRS-3 in lung cancer cells. *J Pharmacol Exp Ther* **287**:366–380.
Sancho V, Di Florio A, Moody TW, and Jensen RT (2011) Bombesin receptor-mediated imaging and cytotoxicity: review and current status. *Curr Drug Deliv* **8**:79–134.

Sancho V, Moody TW, Mantey SA, Di Florio A, Uehara H, Coy DH, and Jensen RT (2010) Pharmacology of putative selective hBRS-3 receptor agonists for human bombesin receptors (BnR): affinities, potencies and selectivity in multiple native and BnR transfected cells. *Peptides* **31**:1569–1578.
Sebhat IK, Franklin C, Lo MM, Chen D, Jewell JP, Miller R, Pang J, Palyha O, Kan Y, Kelly TM, et al. (2010) Discovery of MK-5046, a potent, selective bombesin receptor subtype-3 agonist for the treatment of obesity. *ACS Med Chem Lett* **2**:43–47.
Tokita K, Katsuno T, Hocart SJ, Coy DH, Llinares M, Martinez J, and Jensen RT (2001) Molecular basis for selectivity of high affinity peptide antagonists for the gastrin-releasing peptide receptor. *J Biol Chem* **276**:36652–36663.
Tränkle C, Andresen I, Lambrecht G, and Mohr K (1998a) M2 receptor binding of the selective antagonist AF-DX 384: possible involvement of the common allosteric site. *Mol Pharmacol* **53**:304–312.
Tränkle C, Mies-Klomfass E, Cid MH, Holzgrabe U, and Mohr K (1998b) Identification of a [3H]ligand for the common allosteric site of muscarinic acetylcholine M2 receptors. *Mol Pharmacol* **54**:139–145.
Tsuda T, Kusui T, Hou W, Benya RV, Akeson MA, Kroog GS, Battey JF, and Jensen RT (1997) Effect of gastrin-releasing peptide receptor number on receptor affinity, coupling, degradation, and modulation. *Mol Pharmacol* **51**:721–732.
Uehara H, González N, Sancho V, Mantey SA, Nuche-Berenguer B, Pradhan T, Coy DH, and Jensen RT (2011) Pharmacology and selectivity of various natural and synthetic bombesin related peptide agonists for human and rat bombesin receptors differs. *Peptides* **32**:1685–1699.
Uehara H, Hocart SJ, González N, Mantey SA, Nakagawa T, Katsuno T, Coy DH, and Jensen RT (2012) The molecular basis for high affinity of a universal ligand for human bombesin receptor (BnR) family members. *Biochem Pharmacol* **84**:936–948.
van Westen GJ, Gaulton A, and Overington JP (2014) Chemical, target, and bioactive properties of allosteric modulation. *PLOS Comput Biol* **10**:e1003559.
von Schrenck T, Wang LH, Coy DH, Villanueva ML, Mantey S, and Jensen RT (1990) Potent bombesin receptor antagonists distinguish receptor subtypes. *Am J Physiol* **259**:G468–G473.
Wang LH, Coy DH, Taylor JE, Jiang NY, Kim SH, Moreau JP, Huang SC, Mantey SA, Frucht H, and Jensen RT (1990a) Desmethionine alkylamide bombesin analogues: a new class of bombesin receptor antagonists with potent antisecretory activity in pancreatic acini and antimitotic activity in Swiss 3T3 cells. *Biochemistry* **29**:616–622.
Wang LH, Coy DH, Taylor JE, Jiang NY, Moreau JP, Huang SC, Frucht H, Haffar BM, and Jensen RT (1990b) des-Met carboxyl-terminally modified analogues of bombesin function as potent bombesin receptor antagonists, partial agonists, or agonists. *J Biol Chem* **265**:15695–15703.
Weber HC (2015) Gastrointestinal peptides and itch sensation. *Curr Opin Endocrinol Diabetes Obes* **22**:29–33.
Wold EA and Zhou J (2018) GPCR allosteric modulators: mechanistic advantages and therapeutic applications. *Curr Top Med Chem* **18**:2002–2006.
Wootten D and Miller LJ (2020) Structural basis for allosteric modulation of class B G protein-coupled receptors. *Annu Rev Pharmacol Toxicol* **60**:89–107.
Wootten D, Miller LJ, Koole C, Christopoulos A, and Sexton PM (2017) Allostery and biased agonism at class B G protein-coupled receptors. *Chem Rev* **117**:111–138.
Xiao C and Reitman ML (2016) Bombesin-like receptor 3: physiology of a functional orphan. *Trends Endocrinol Metab* **27**:603–605.

Address correspondence to: Dr. Robert T. Jensen, Digestive Diseases Branch, NIDDK, NIH, MSC 1804, Building 10, Room 9C-103, 10 Center Drive, Bethesda MD 20892-1804. E-mail: robertj@bdg10.niddk.nih.gov